

N90-26467

EXPERIMENT K-6-13

MORPHOLOGICAL AND BIOCHEMICAL EXAMINATION OF HEART TISSUE

- PART I: EFFECTS OF MICROGRAVITY ON THE MYOCARDIAL
FINE STRUCTURE OF RATS FLOWN ON COSMOS
1887 - ULTRASTRUCTURE STUDIES
- PART II: CELLULAR DISTRIBUTION OF CYCLIC AMP-
DEPENDENT PROTEIN KINASE REGULATORY
SUBUNITS IN HEART MUSCLE OF RATS FLOWN ON
COSMOS 1887

Principal Investigator:

D.E. Philpott
NASA Ames Research Center
Moffett Field, California 94035

Co-Investigators:

K. Kato, J. Stevenson,
NASA Ames Research Center
Moffett Field, California 94035

J. Miquel
Linus Pauling Institute of Science and Medicine
Palo Alto, California 94306
University School of Medicine
Alicante, Spain

M.I. Mednicks
Department of Molecular Biology
Northwestern University Medical School
Chicago, Illinois 60611

W. Sapp
Tuskegee University
Tuskegee, Alabama 36088

I.A. Popova, L.V. Serova
Institute of Biomedical Problems
Moscow, USSR

EXPERIMENT K-6-13

PART I: EFFECTS OF MICROGRAVITY ON THE MYOCARDIAL FINE STRUCTURE OF RATS FLOWN ON COSMOS 1887 - ULTRASTRUCTURE STUDIES

D. Philpott, I. Popova, L. Serova, K. Kato, J. Stevenson, J. Miquel, and W. Sapp

SUMMARY

The left ventricle of hearts from rats flown on the Cosmos 1887 biosatellite for 12.5 days was compared to the same tissue of synchronous and vivarium control animals maintained in a ground based laboratory. The volume density of the mitochondria in the myocardium of the space-flown animals was statistically less ($p < 0.01$) than that of the synchronous or vivarium control rats. Exposure to microgravity resulted in a certain degree of myocardial degeneration manifested in mitochondrial changes and accumulation of myeloid bodies. Generalized myofibrillar edema was also observed.

INTRODUCTION

Vascular deconditioning, which is an important medical problem, is recognized as one of the key concerns of space flight research. This loss of physiological performance of the circulatory system is accompanied by disuse muscle atrophy triggered by the reduced functional load of the musculo-skeletal system in the microgravity environment. Animal models are often used to examine disuse atrophy because they are more amenable to the morphological and biochemical research needed to unravel the mechanisms of muscle breakdown. Using these models, we can design preventive countermeasures.

Although early Soviet space flight data suggested that rat heart was insensitive to weightlessness (Oganessyan and Eloyan, 1979), more recent studies have shown that subcellular alterations occur in the rat heart following exposure to space microgravity or on-the-ground immobilization (Baranski, 1983). An examination of rats from a 22-day flight, sacrificed 4.5-9 hrs postflight, revealed changes in capillaries and veins consisting of edema of the endothelial cytoplasm, appearance of myeloid bodies and swelling of mitochondria. In the cardiomyocytes, exposure to microgravity results in an increase in the number of lipid droplets and an increase in the amount of extramitochondrial glycogen. Philpott et al. (1985, 1987) also reported alterations in the heart following exposure to space microgravity on Space Lab-3, including a significant decrease in volume density of the mitochondria, loss of microtubules and increases in lipid droplets and glycogen.

Rat heart mass decreased 4.26% and oxygen consumption decreased from 62 mm squared to 38 mm squared/100 mg/hr after 120 days of restraint (Kovalenko et al. 1971). Electron microscopy revealed non-uniform swelling and a decrease in the number of cristae of the mitochondria and changes in their patterns of orientation (Kovalenko et al. 1970, Kovalenko et al. 1972). The endothelium of the capillaries exhibited swelling and impairment of the cell membrane structure. Mailyan et al. (1970) induced hypokinesia by exercise restriction which resulted in reduced heart function accompanied by a clear decrease in mass and changes in the ultrastructural elements on which biological oxidation processes are dependent. Shtykhno and Udovichenko (1978) showed a decrease in the number of true capillaries, appearance of nonfunctioning empty vessels, and an opening of arteriovenular shunts.

In another study on male rats that were restrained for 120 days electron microscopy revealed, by day 14, an increase in the number of and a decrease in the size of mitochondria (Romanov, 1976). At days 45-60, size and number of mitochondria appeared normal, but by the 120th day both size and number of mitochondria were greater than in control non-restrained animals. The reasons for these changes are unknown and further research is needed to clarify the adaptive mechanisms involved in the response of the heart tissues to altered gravity.

Stereological methods were used to study skeletal and heart muscle changes after 30 days of hypokinesia (Nepomnyashchikh et al. 1985). Forty-eight male rats were confined in cages, allowing virtually no movement. The ratio of muscle to connective tissue in the myocardia decreased (connective tissue proliferation), the relative volume of intracellular material increased (edema), and the microcirculatory bed was altered, leading to a degrading of metabolic processes. Both morphological and stereological analysis revealed myocardial atrophy. Philpott et al. (1984) demonstrated a significant decrease in volume density of mitochondria in the rat deep quadriceps (6 & 9-days suspension) and superficial quadriceps (12-days suspension) accompanied by an increase in the number of mitochondria and a decrease in the perimeter of the mitochondria.

Microtubules perform a cytoskeletal role in cells, providing for structural integrity and intracellular transport. It is believed that microtubules have an orienting function for intracellular structures in muscle, especially the myofibrils. Cartwright and Goldstein (1985) have shown that the number of microtubules in the rat heart increase for the first nine postnatal days and then decrease to a steady state. These authors have observed a specific pattern in the number of microtubules, relative to increases in the number of myofibrils in both heart and soleus muscle. This indicates that the microtubules provide an orienting function for myofibrils. The relatively stable state of the microtubules, which are observed in the adult heart, tend to support a static cytoskeletal role for microtubules in a normal functioning heart. Warren (1968) demonstrated that the breakdown of microtubules by colchicine disrupts the orderly arrangement of myofilament bundles in regenerating frog skeletal muscle. Cartwright and Goldstein (1985) believe that reduced microtubule density reflects a decreased necessity for scaffolding after well-oriented, densely packed myofilament bundles are established. Only the microtubules required for growth remain.

Male rats were flown for 7 days on Space Lab-3 and sacrificed 12 hours after recovery of the shuttle. Philpott et al. (1985) observed a decrease in microtubules in rat heart tissue. This would suggest a decreased need for scaffolding as hearts have been shown to lose mass under simulated weightlessness. An increase in number of microtubules in response to stress-induced hypertrophy has been shown by Samuel et al. (1983), and these microtubules temporarily reorganize into bundled arrays. Little is known about the assembly and breakdown of heart microtubules. In rats flown on Space Lab-3, ultrastructural changes include an increase in glycogen and small lipid droplets, and a decrease in cytoskeletal tubules compared to controls.

The present study expands our previous research in which male Wistar rats were flown on Space Lab-3 (SL-3) for seven days (Philpott et al., 1985). In agreement with the earlier research, we have found that exposure to microgravity results in a number of myocardial changes including, myofibrillar edema, loss of cytoskeletal tubules, mitochondrial disorganization and accumulation of glycogen and lipid.

MATERIALS AND METHODS

All of the animals were male rats of the Czechoslovakian-Wistar strain, weighing about 325g at launch time. The biosatellite Cosmos 1887 flight lasted 12.5 days, and landed in Siberia. The rats were transported by bus, airplane and van to the laboratory in Moscow, and were sacrificed two days after recovery. Tissue was obtained from five space flown rats for the study of the effects of microgravity on the myocardium. Ten rats of the same age and sex served as controls. Of these, five animals were kept under normal laboratory conditions ("vivarium controls") and five were

maintained under the same conditions as the space-flown rats with the exception of no microgravity ("synchronous controls"). The hearts were removed as quickly as possible after sacrifice and immersed in cold saline (Fig. 1) to slow the metabolic rate during dissection (Kato, et al., 1987). The left ventricles were removed and cut into four parts. Two of the pieces were placed into cold Triple Fix (Philpott, et al., 1980); the remaining two pieces were frozen in liquid nitrogen and later transferred to dry ice for transportation to Ames Research Center. All tissues were placed in screw top teflon tubes to facilitate handling and transportation. Upon arrival in the United States, the tissue in Triple Fix was immersed in 1% osmic acid plus 1% $K_3Fe(CN)_6$ for one hour (McDonald, 1983), dehydrated with ascending concentrations of acetone, infiltrated with epon araldite, embedded, sectioned and stained for electron microscopy. A minimum of 100 electron micrographs from each animal were taken in a Philips-300 transmission electron microscope. Volume density of the mitochondria was determined by point counting, as described by Weibel (1969), using 8×10 micrographs at a magnification of 27,500X.

RESULTS AND DISCUSSION

The mean animal weights at recovery were: Flight = 303.2gm (S.E. 2.4), Synchronous = 349.0gm (S.E. 5.8), and Vivarium = 342.0gm (S.E. 7.7). Point counting on random micrographs to determine the volume density of mitochondria, revealed a significant decrease in volume density in the flight-animal tissue, compared to the controls. Some of the myofibrils in the flight samples exhibited degeneration of the mitochondria and formation of myeloid bodies. Generalized edema was present in the myofibrils showing degeneration. There was some increase in glycogen and lipid in the myocardium of Cosmos 1887 flown rats but not as markedly as in animals exposed to microgravity in the Shuttle Spacelab (SL-3) or subjected to immobilization-suspension.

Previous research suggests that microgravity leads to degenerative structural changes and biochemical adaptations involving storage of lipid and glycogen. In this study, the accumulation of these substances was not as evident as in previous space flights, which may be due to difficulties during recovery resulting in a 42 hour fasting period prior to sacrifice. Glycogen increase is seen in Fig. 2 and Fig. 3 where some increase in lipids is also observed.

Structural changes seen in the Cosmos flown rats include some loss of microtubules and fibrillar edema that may be linked to tissue breakdown, with a concomitant increase in osmotic pressure and fluid entry into the cells. Intermittent areas of missing protofibril (actin, myosin filaments) were observed in cross sections of flight tissue which is indicative of muscle degradation (Fig. 4). Another structural change seen is mitochondrial breakdown, which occurs both in space flown and immobilized animals. (Fig. 5). A number of fibers in the flight tissue exhibited super contraction (Fig. 3). While preparative technique can contribute to this, the super contraction was not evident in the controls. It is possible that mitochondrial breakdown is releasing calcium which may contribute to the contracted state. These changes can be compared to the vivarium and synchronous control tissues (Figs. 6, 7). Point counting of the mitochondria in the left ventricle resulted in a mean of 39.9 for the vivarium, 38.9 synchronous and 32.5 for the flight tissue. The t-test shows a significant difference between the flight and both the vivarium and synchronous controls of < 0.01 , but no significant difference between the vivarium and synchronous controls (Fig. 8). It is clear that the volume density of the mitochondria in the flight group was reduced by a significant amount.

Since the sympathetic nervous system exerts a trophic influence on the biosynthesis of myofibrils and mitochondria (Joseph and Engel, 1980), a decreased sympathetic activity, under conditions of microgravity or immobilization, could play a key role in mitochondrial degeneration. Mitochondrial damage could also result from changes in intracellular oxygen tension. According to Fedorov and Shurova (1973), immobilized rabbits show capillary alterations which might impair the delivery of oxygen and nutrients to the myocardial cells. This would decrease the ATP

synthesis in all or some of the mitochondrial populations, and since ATP is needed for mitochondrial maintenance and replication, the end result would be unrepaired mitochondrial loss (Tzagoloff, 1982). Capillary alterations were also seen in the flight tissues (Fig. 9) in the form of numerous endothelial invaginations projecting into the lumen of the capillaries.

The above hypothesis is supported by the fact that alterations in the supply of oxygen and nutrients to the organelles result in fine structural and biochemical changes in the mitochondria of ischemic or anoxic myocardium (DeGasperis et al., 1970; Delatglesia and Lumb, 1972; Ferrans and Roberts, 1971; Rouslin et al., 1980; Taylor and Shaikh, 1984). Both sympathetic and oxygen-mediated mechanisms may underly the organelle changes since the decline in sympathetic nervous activity may also influence mitochondria through its effect on myocardial blood perfusion (Popovic, 1981).

The present data support the view that an optimum work load imposed on the heart, i.e. moderate physical exercise at normal Earth gravity, is essential for preservation of mitochondrial structure and function (Miquel et al., 1980; Miquel 1982). At present, our understanding of the causes and basic mechanisms of cardiovascular deconditioning is inadequate. Changes/lesions have been observed in the cardiovascular tissue. This may provide information which will be of relevance and importance for the well-being of individuals involved in prolonged space flight under conditions of microgravity and /or significantly restricted or diminished physical activity.

ACKNOWLEDGMENTS

We wish to thank Michael Penn for his contribution in preparing statistical material at Ames Research Center for this manuscript.

REFERENCES:

1. Baranski S., Subcellular investigation of the influence of real and modulated weightlessness upon performance and regeneration processes in muscular tissues. *The Physiologist* 26:41, 1983.
2. DeGasperis, C., A. Miani, and R. Donatelli. Ultrastructural changes in human myocardium associated with ischemic arrest. *J. Mol. Cell. Cardiol.* 1:169, 1970.
3. Delatglesia, F. A. and G. Lumb. Ultrastructural and circulatory alterations of myocardium in experimental coronary artery narrowing. *Lab. Invest.* 27:17, 1972.
4. Fedorov, I. V. and I. F. Shurova. Content of protein and nucleic acids in the tissue of animals during hypokinesia. *Kosmicheskaya Biologiya i Meditsina.* 7:17, 1973.
5. Ferrans, V. J. and W.C. Roberts. Myocardial ultrastructure in acute and chronic hypoxia. *Cardiol.* 56:144, 1971.
6. Joseph, J.J. and B. T. Engel. Nervous control of the heart and cardiovascular system. *Aging.* 12:101, 1980.
7. Kato, K., A. Baloun, and D.E. Philpott. Effect of supergravity on the areas of lipid droplets and mitochondria in the heart left ventricle. *J. Ultrastruc. Res.* 69:350, 1979.
8. Kato, K., D. Philpott and J. Stevenson. A simple method to improve heart fixation with ice water. *J. Elect. Micros. Tech.* 7:(2), 133, 1987.
9. Kovalenko, Ye. A., V. L. Popkov and Yu. I. Kondrat'yev. *Pathological Physiology.* 6: 3-8, 1979.

10. Kovalenko, Ye. A., V. L. Popkov and E. S. Mailyan. *Kosmicheskaya Biologiya I Meditsina*. 4: 3-8, 1971.
11. Kovalenko, Ye. A., Yu. S. Galushko and I. A. Nitochkina. *Space Biol. and Aerospace Med.* 1: 125-129, 1972.
12. Mailyan, E. S., L. I. Grinberg and Ye. A. Kovalenko. *Adaptatsiya K Myshechnoy Deyatel'nosti I Gipokinezii*. Novosibirsk, 111- 113, 1970.
13. McDonald, K. OsFeCN-uranium staining improves microfilament preservation and membrane visualization in a variety of cell types. *J. Ultrastructural Res.* 86: 107-118, 1984.
14. Miquel, J., A. C. Economos, J. Fleming, and J. E. Johnson, Jr. Mitochondrial role in cell aging. *Exp. Gerontol.* 15: 575, 1980.
15. Miquel, J. Comparison between the weightlessness syndrome and aging. In: *Space Gerontology* (J. Miquel and A. C. Economos, Eds.), NASA, Washington, D.C., 1982.
16. Nepomnyashchikh, L. M., L. V. Kolesnikova, G. I. Nepomnyashchikh. Myocardial tissue organization in rats under hypokinesia (a stereological investigation), *Arkhir Anatomii, Gistologii I Embriologii*. 88:(1)57-62, 1985.
17. Oganessyan, S. S., and M. A. Eloyan. Cathepsin activity of skeletal muscle and myocardial myofibrils after exposure to weightlessness and accelerations. *Kosmicheskaya Biologiya I Aviakosmicheskaya Meditsina* 45, 38, 1979.
18. Philpott, D.E., R. Corbett, C. Turnbull, S. Black, D. Dayhoff, J. McGourty, R. Lee, G. Harrison and L. Sovick. Retinal changes in rats flown on Cosmos 936: A cosmic-ray experiment. *Aviat. Space and Environ. Med.* 51:556, 1980.
19. Philpott, D. E., J. Miquel, M. Wilke and M. Ornelas. Stereological changes in skeletal mitochondria during disuse atrophy. *International Cell Biol. Special Issue.* 509, 1984.
20. Philpott, D. E., A. Fine, K. Kato, R. Egnor, L. Cheng and M. Mednieks. Microgravity changes in heart structure and cyclic AMP metabolism. *Suppl. to The Physiologist* 28:(6),S209, 1985.
21. Philpott, D. E., K. Kato and M. Mednieks. Ultrastructure and cyclic AMP mediated changes in heart muscle under altered gravity conditions. *J. Mol. Cell Cardiol.* 19:(IV), S61, 1987.
22. Romanov, V. S. Quantitative evaluation of ultrastructural changes in rat myocardium during prolonged hypokinesia. *Space Biol and Aerospace Med.* 10, 74, 1976.
23. Rouslin, W., J. MacGee, A. R. Wesselman, R. J. Adams and S. Gupte. Mitochondrial cholesterol in myocardial ischemia. *J. Mol. Cell Cardiol.* 12:1475, 1980.
24. Samuel, J. L. The microtubule network of cardiac myocytes during adaptive growth. *J. Mol. Cell Cardiol.* 15:(4) 38, 1983.
25. Shtykhno, Yu. M. and V. I. Udovichenko. *Vest. Akad. Med. Nauk SSSR.* 2: 68-71, 1978.
26. Taylor, I. M. and N. A. Shaikh. Ultrastructure changes of ischemic injury due to coronary artery occlusion in the porcine heart. *J. Mol. Cell. Cardiol.* 16: 79, 1984.

27. Tzagoloff, A. *Mitochondria*. Plenum Press, New York, 244, 1982.

28. Warren, R. H. The effect of colchicine on myogenesis in vivo in *Rana pipiens* and *Rhodnius prolixus* hemiptera. *J. Cell. Biol.* 39: 544-555, 1968.

29. Weibel, E.R. Stereological principles for morphometry in electron microscopy cytology. *Int. Rev. Cytol.* 26: 235, 1969.

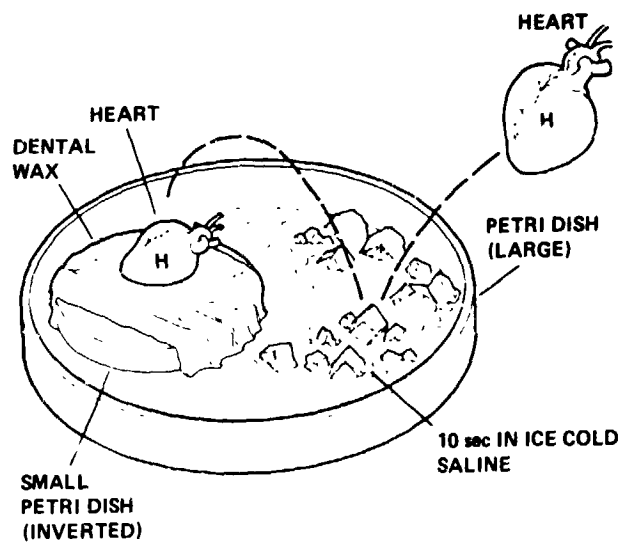


Fig. 1. Diagram of heart tissue preparation showing how the heart is quickly cooled after sacrifice, in order to decrease metabolism-linked autophagic breakdown prior to fixation.

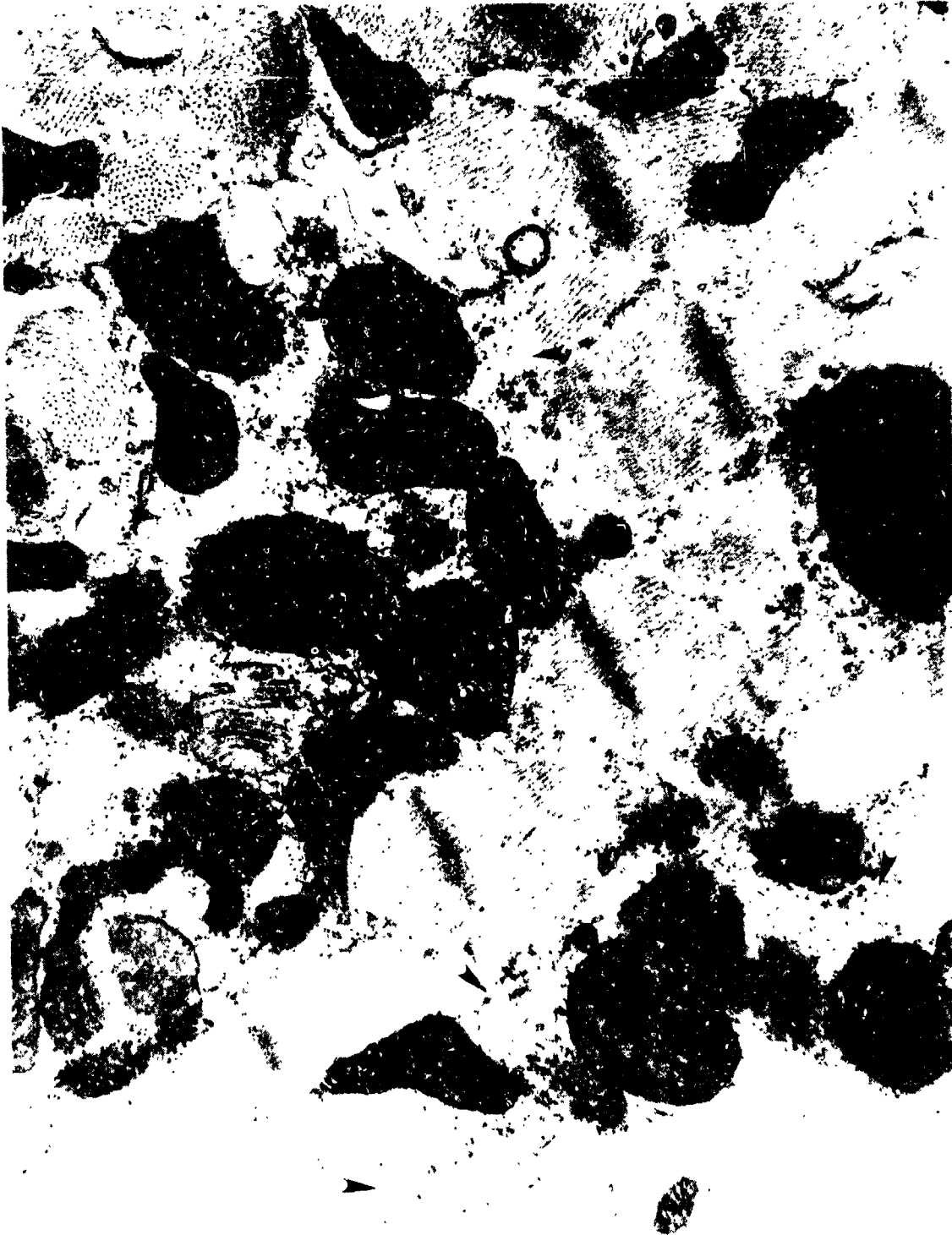


Fig. 2. Abundant glycogen deposits (arrows) in the myocardium of a space-flown rat. 27,500X.

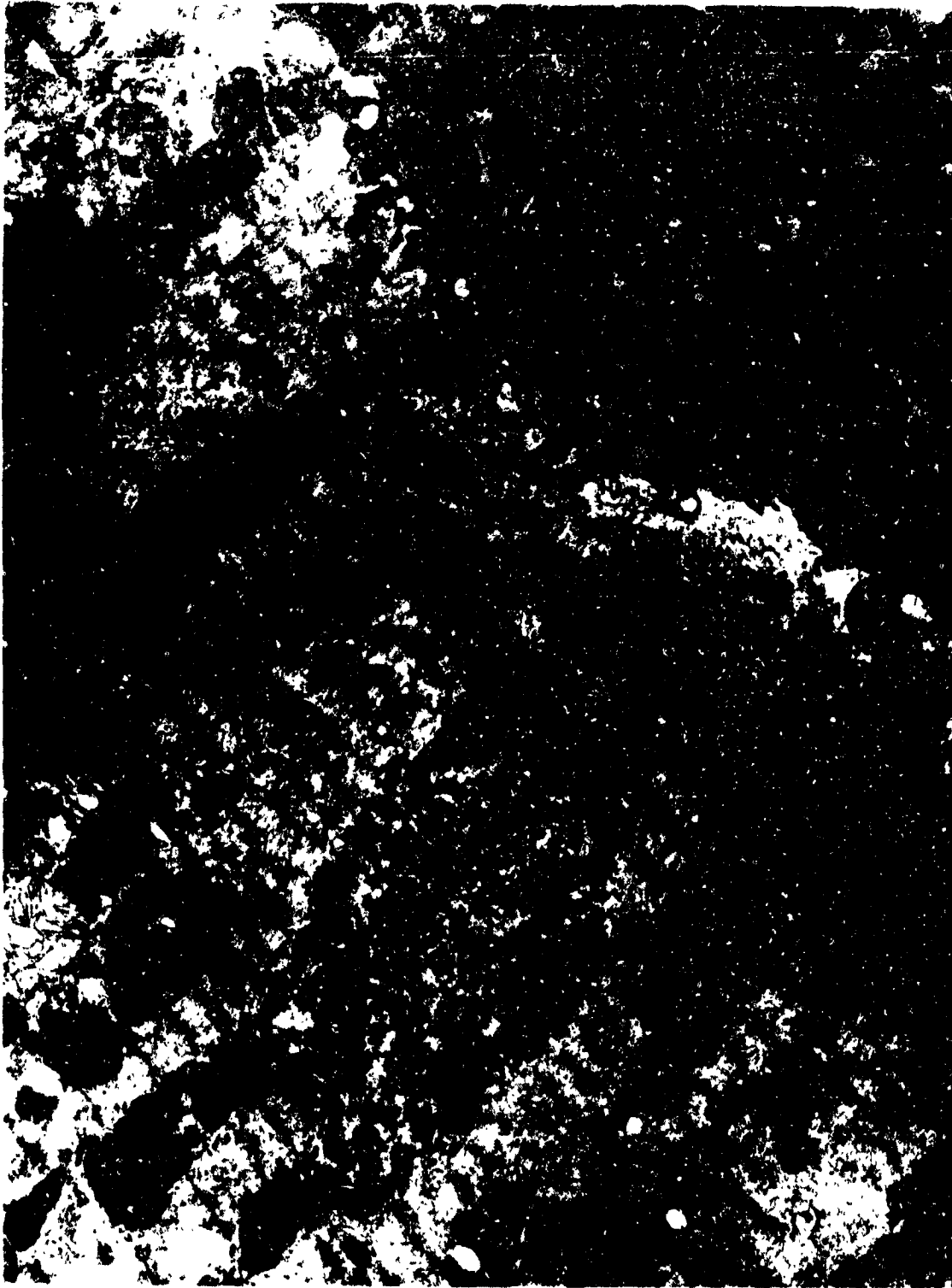


Fig. 3. A super contracted fiber connecting to a normal fiber was seen in the flight tissue. Note the lighter staining mitochondria in the super contracted fiber, increased glycogen and swollen mitochondria (arrow). 19,500X.



Fig. 4. Filaments are occasionally missing (arrows) in cross sections of the left ventricle of a flight rat. 130,000X.



Fig. 5. Evidence of mitochondrial alteration (arrow) in the left ventricle of a space-flown animal. 127,500X.

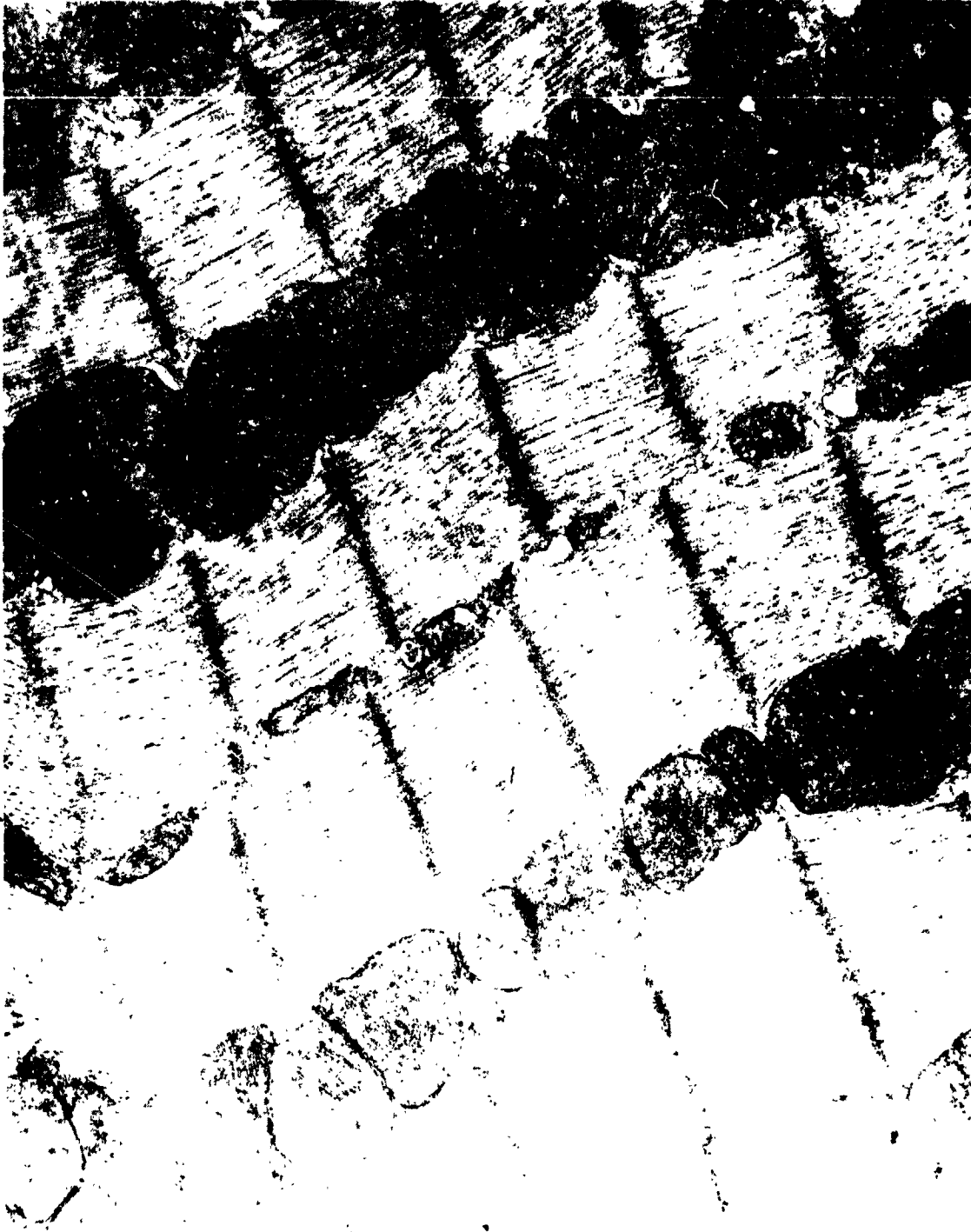


Fig. 6. Vivarium control left ventricle tissue. Note excellent preservation. 27,500X.

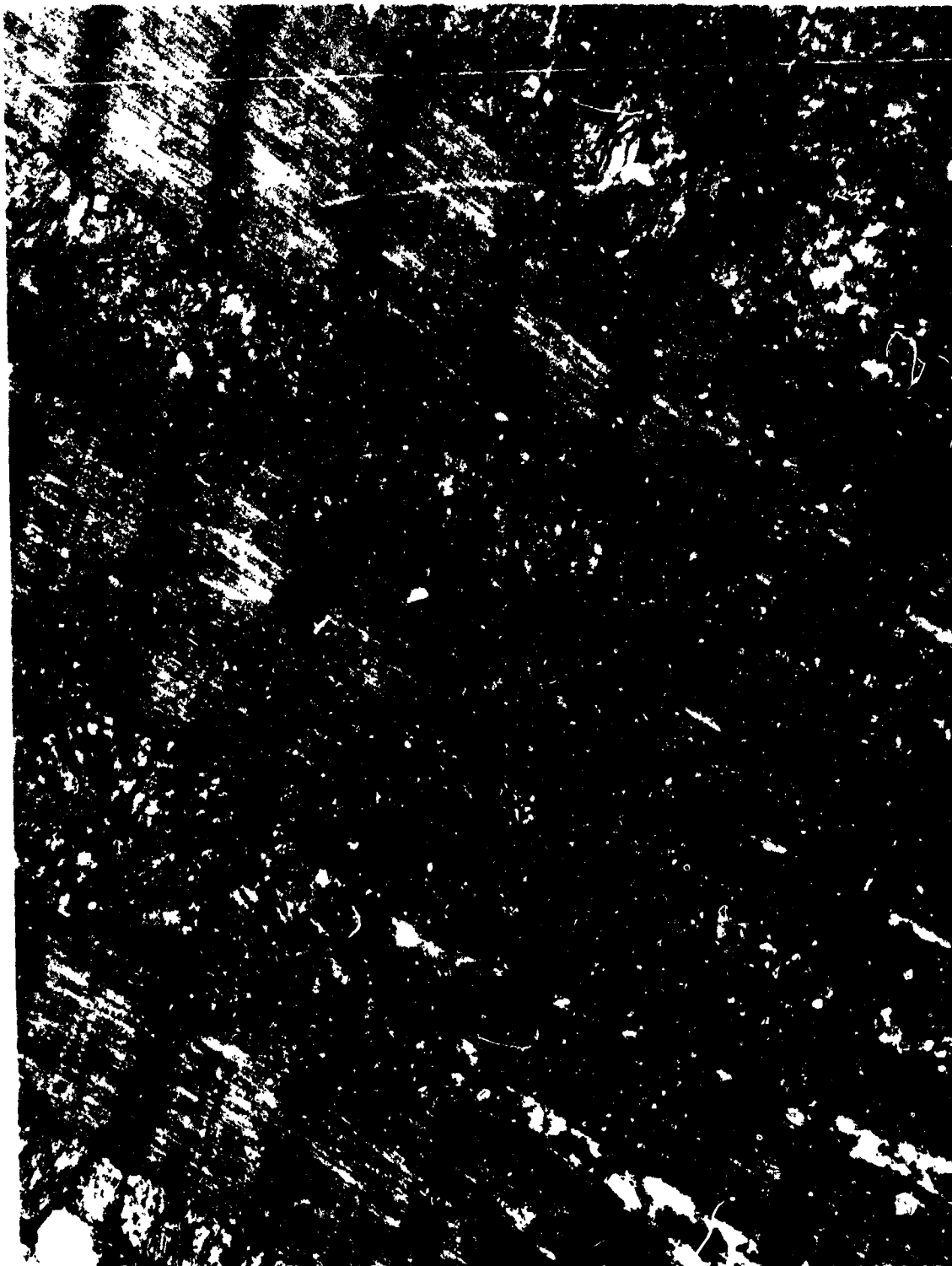


Fig. 7. Synchronous control left ventricle. Note similarity to vivarium control. 27,500X.

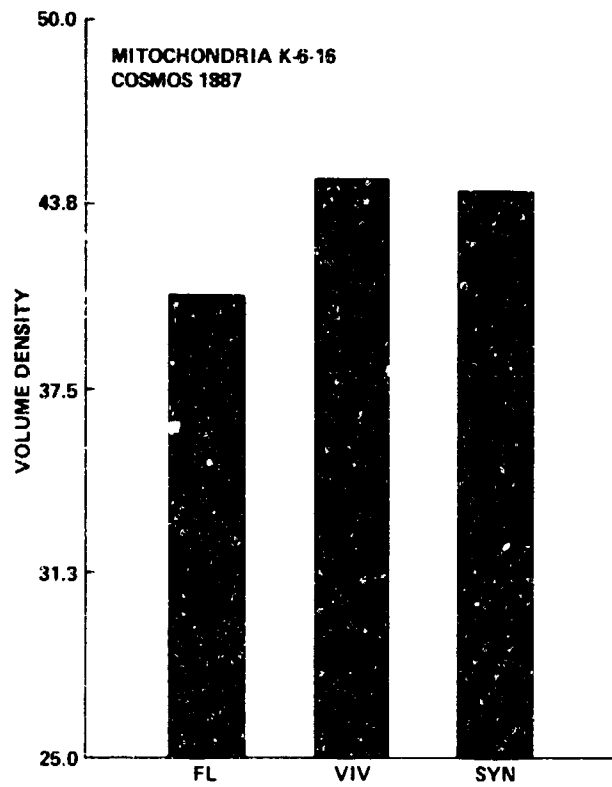


Fig. 8. Volume density of mitochondria in the myocardium of rats flown in the Cosmos 1887 biosatellite.



Fig. 9. Ultrastructural alterations seen in the left ventricle of a flight rat. Note the endothelial projections in the lumen of the capillary. 141,000X.

EXPERIMENT K-6-13

PART II: CELLULAR DISTRIBUTION OF CYCLIC AMP-DEPENDENT PROTEIN KINASE REGULATORY SUBUNITS IN HEART MUSCLE OF RATS FLOWN ON COSMOS 1887

M. Mednieks

SUMMARY

In this study, the cellular compartmentalization and biochemical localization of regulatory (R) subunits of cyclic AMP-dependent protein kinase (cAPK) of ventricular heart tissue from rats obtained from the COSMOS 1887 were determined. Photoaffinity labeling with a [³²P]-8-azido analog of cyclic AMP, electrophoretic separation of the proteins was followed by autoradiographic identification of the subcellular fraction in which the labeled R subunits are localized. Similarly, antibodies to R subunits were prepared and employed in an immunogold electron microscopic procedure to directly visualize cellular compartmentalization of the cAPK R subunits. Our results show that protein banding patterns in both the cytoplasmic fraction and in a fraction enriched in chromatin-bound proteins showed some individual variability in tissues of different animals, but exhibited no changes that can be attributed to the flight. Examination of cellular localization of the isotopically labeled R subunits of cAPK isotypes showed no change in the distribution of RI in either the soluble or particulate fractions whereas the presence of RII in the particulate subcellular fraction as well as in the regions of nuclear chromatin was greatly decreased in tissues from rats in the flight group when compared to controls. Identical results were obtained in comparable tissues obtained from the U.S. Space Lab 3 (SL-3) mission. These findings indicate that a major catecholamine hormone regulated mechanism in cardiac tissue is altered during some aspect of space travel.

INTRODUCTION

Samples were obtained from the Cosmos 1887 flight and tested with respect to cellular compartmentalization and biochemical localization of cyclic AMP-dependent protein kinase (cAPK). Results were compared to the findings of similar analyses performed using materials obtained from the U.S. Space Lab 3 (SL-3) mission.

The study was undertaken in order to gain insight into the mechanistic aspects of cardiac changes that both animals and humans undergo as a consequence of space travel (1,2). Cardiac hypertrophy and cephalad fluid shifts have been observed after several days of actual or simulated weightlessness and raise concerns regarding the functioning of the heart and circulatory system during and after travel in space (3,4,5).

A number of physiologic changes, attributed to space travel conditions in experimental animals and in humans, can be the consequence of increased circulating levels of catecholamine hormones. On a cellular level such responses are of two types and have been studied in other tissues (6,1). The immediate effects, which are generally transient in nature and the later or delayed effects which appear to be longer lasting, involve gene regulation and have longer or unknown recovery periods. The second type of reaction is of considerable practical concern and is addressed in this study.

A series of events occur as a consequence of stimulation of cardiac muscle tissue by catecholamine hormones: receptor binding at the cells' surface is followed by activation of adenylate cyclase in the plasma membrane resulting in increased cyclic AMP production, activation of cAPK, and is

played out as the intracellular signal processing which is a function of the activity and distribution of cAPK.

The two basic steps in intracellular protein phosphorylation which are mediated by cAMP are: a) holoenzyme dissociation and b) regulatory (R) and catalytic (C) subunit activity:



where R·C is the catalytically inactive holoenzyme, R·cAMP represents regulatory subunits, with binding sites occupied. Two isotypes (I and II) of cAPK have been found which have identical C subunits, but differing R subunits, RI and RII (8,9).

An advantage in this experimental design is the specificity of the cAPK R subunits: they are the only known eukaryotic cAMP-receptor or cAMP-binding proteins (10). Labeled R subunits serve as radioactive probes to search for cytosolic or nuclear cellular localization of cAPK. Antibodies generated to R subunits served as independent means of immunocytochemical localization.

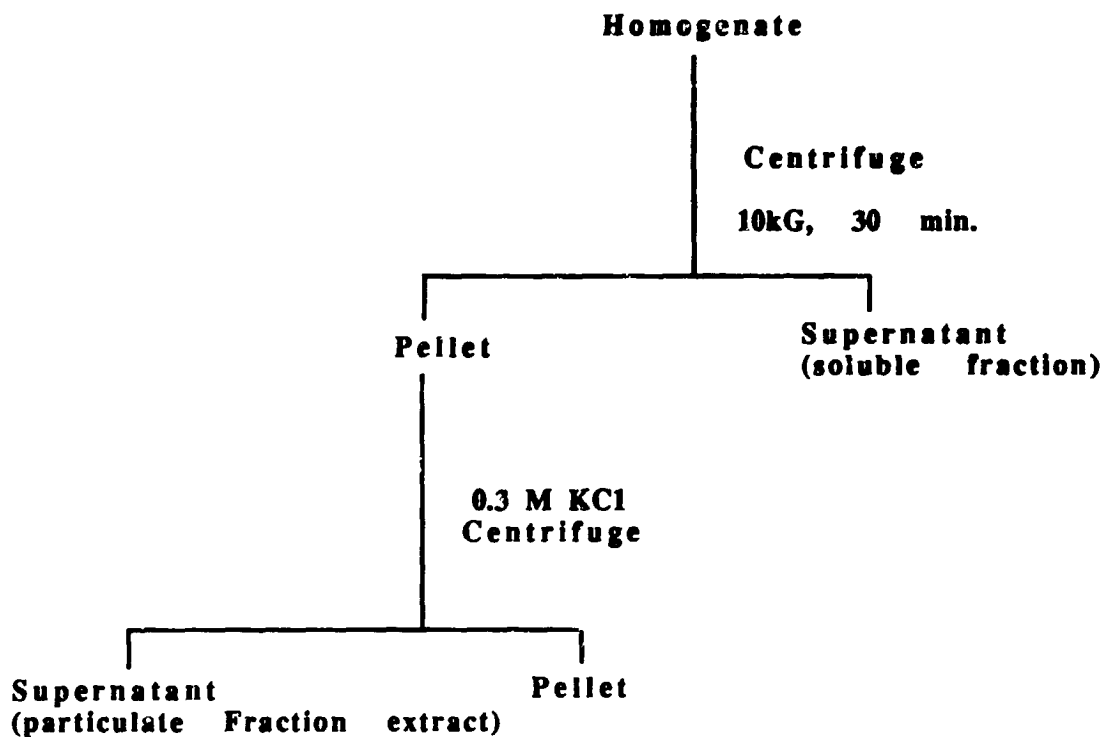
The fundamental finding of this study is the apparent decrease of nuclear cAPK RII. This is consistent with previous results using tissues from rats flown on SL-3.

MATERIALS AND METHODS

The initial experiments were carried out at NASA, Ames, Moffett Field, but were repeated and concluded at Northwestern University in Chicago. While the methods employed were identical, aliquots of the samples used, equipment, solutions and individuals carrying out the procedures varied. This repetition was undertaken to ensure that the results were reproducible.

Tissue Homogenization and Cell Fractionation

Heart (left ventricle) tissue pieces were weighed and a 0.05M Tris, pH 7.5 buffer containing 0.06M EDTA, 0.005M MgCl₂ and 0.001M benzamidine and phenyl methyl sulfonyl flouride (PSMF) was added to make a 15% (w/v) homogenate. The tissue pieces were disrupted using a Polytron probe at the number 5 setting with two 30 second bursts. These and all subsequent operations using the tissue homogenates were carried out at 4 °C. The homogenates were centrifuged at 10 kG for 30 minutes and the supernatant solution was removed and saved and subsequently designated the soluble fraction. The particulate fraction was suspended in the same volume as the original homogenate in 0.30M KCl containing the homogenization buffer. The samples were mixed using a Vortex mixer at the maximum setting, allowed to stand for 30 minutes, mixed again and centrifuged at 10kG for 30 minutes. The supernatant of this centrifugation was saved and is referred to as the particulate fraction extract. The tissue fractionation steps are shown schematically as follows:



Heart muscle tissue samples from each individual animal were homogenized separately, and all analyses were carried out on these samples. Some individual variability could be observed, so that if tissues were pooled and only groups, i.e., control, simulated and flight were analyzed, the individual differences of one animal might seriously alter the average value of the whole group.

Photoaffinity Labeling.

Photoaffinity labeling was carried out using a method modified from Hoyer et al (8), as described previously (11). Duplicate aliquots containing 50 μ g total protein were taken from the homogenate, the soluble fraction and the particulate fraction extract and incubated with 5 μ Ci each of [32 P]-8-azido cyclic AMP ([32 P]-8-N₃-cAMP) in an equal volume of buffer containing 0.25M KCl, 0.002M Tris, pH 7.6, 0.001M EDTA for 30 minutes at 4 °C, in the dark. Photolysis was carried out using a mineralite UV lamp at a wavelength of 250 nm at a distance of 5 cm. The samples were then treated with activated charcoal and centrifuged.

Total incorporation of the labeled analog was measured by taking duplicate aliquots of samples representing 0.1 mg tissue adding trichloroacetic acid to the concentration of 5% and allowed to form a precipitate overnight in the cold. The precipitates were collected, solubilized and duplicate aliquots were counted using a liquid scintillation counter.

Electrophoresis and Autoradiography.

Sodium dodecyl sulfate polyacrylamide gel electrophoresis (SDS-PAGE) was carried out using a mini-gel apparatus (Hoffer Instruments). Standard procedures, described before (14), were employed in preparing the electrophoresis separations. The proteins were then electrophoretically transferred to nitrocellulose by Western blotting. Autoradiography was carried out by exposing either dried gels or Western blots to X-ray film to detect the radioactively labeled protein bands. Colored standards (Amersham Rainbow markers) were used to determine relative mobilities of standard proteins and to identify the radioactively labeled R subunits.

Electron microscopic immunogold labeling.

Polyclonal antibody reactive with cAPK RI was used for postembedding cytochemical immunogold labeling of rat heart and testis tissues from the Cosmos flight. The serum was an early positive bleeding and has not been affinity purified. The serum was used only to test for normal intracellular RI distribution. Animal handling was in accordance with NIH guidelines. Procedures for immunolabeling were modified from those of Roth and his associates and from Bendayan and have been described before (19). Dilutions of antibody were 1:200 and 1:400. The higher dilution was used to test specificity by antigen inhibition. All quantitative procedures were subjected to standard statistical analysis and all effects on the tissue of flight animals were compared to those of vivarium and simulation controls.

RESULTS

Protein Concentration and Banding Patterns

Rat heart ventricle tissue pieces were disrupted and a soluble fraction and an extract of the particulate fractions were prepared. Tissues from each individual animal were homogenized separately and were subsequently analyzed on an individual basis. The reason for this procedure is that either subtle differences between experimental and control groups might be missed by examining a single combined sample or conversely, a single tissue piece with extremes in variability may impart a disproportionately great effect. When individual samples are examined they may well be explained by some special condition in one animal (since log-on data from COSMOS are available, e.g., Flight Animal #10 had a significant weight loss, compared to controls, and showed an atypical banding pattern [Figure 3, lane 8]). Additionally, as further flight data become available, accumulating a collection of banding patterns may yield statistically significant information as to possible differences or consistencies, and may become important if heart muscle changes undergoes during space flight.

Electrophoretic separation under denaturing conditions was carried out to examine the protein banding patterns of the flight animal tissues and to compare them to the simulated series and to various controls. Qualitatively, the protein banding patterns were alike for all groups. Densitometric analyses revealed individual differences from animal to animal, but no consistently observed differences between the flight animal tissues when compared to either the tissues of the rats from simulation experiments or to the control group (Fig. 1).

Weight per volume samples (tissue weight in mg/vol buffer to make a 15% homogenate) were prepared and homogenized. Protein concentrations of the soluble fraction and of the extracted particulate fraction were determined by colorimetric measurements and by densitometric analysis of the individual banding patterns (Table I and Figure 1). Table I shows that protein concentrations were the same in the majority of samples (within experimental error) so that only minor adjustments in volume had to be made in pipetting assay solutions of identical concentration with respect to total protein content. Similarly, representative densitometry patterns are shown in Fig. 1 (control A, and simulation B) where the same protein concentration is apparent as the number of peaks, and as the sum of the total area of the peaks. The individual peak heights did vary from animal to animal. No consistent pattern, however, could be correlated with the flight or with either of the control groups.

The protein banding patterns of the soluble fractions of the tissue extracts differ significantly from the banding patterns of the particulate fraction extracts. No differences, however, were observed between control, simulated or flight animal cell fractions (Fig. 1A, 2A, and 3A and in densitometry in Fig. 1). Individual differences between minor bands and some major bands were seen mainly in the soluble fraction banding patterns, but no correlation could be made with either flight or

simulation conditions. Similar observations were previously made in studying cAMP-binding protein distribution on the heart muscle of rats after chronic stimulation with isoproterenol (in press).

Affinity labeling with Azido Cyclic AMP

The binding of an isotopically labeled azido analog of cyclic AMP to its receptor protein (cAPK R subunits) was determined by performing the binding assay, measuring the total incorporation into protein, followed by electrophoretic separation of RI and RII and determining their relative photoaffinity labeling. Fig. 3. shows photoaffinity labeling of the soluble fraction of 4 control and 4 flight animal heart muscle tissues. There is no difference between the groups in total binding of the cAMP analog. Similarly, (not shown) when flight, simulation, and control group labeling is compared, no consistent difference is shown. The R subunit in cytosol is predominantly of the type I isozyme and is indicated in Fig. 3 and verified in the distribution of gold particles bound to antiserum reactive with rat liver RI (Fig. 5A and B). Some azido-labeled RII was observed and it is not clear whether an entry in the photoaffinity label of RII from flight animals in the soluble fraction is present. Extensive analyses of several concentrations and incubation times have to be carried out to ascertain this. At present, the conclusion is that no differences are found in the affinity label (of RI) in the soluble fractions of heart tissues when comparing flight and control samples.

Significant differences in photoaffinity labeling, however, are consistently found in the particulate fraction extracts: less azido cAMP is bound to flight than to control animal RII (Fig. 4 A and B). Banding patterns (Fig 4A) and an autoradiogram (Fig. 4B) are shown side by side to demonstrate first, that equal amounts of protein were photoaffinity labeled and applied to each lane of the electrophoresis gel and second to demonstrate the unequivocal specificity of cyclic AMP binding to R subunits. It should be noted that while the banding pattern exhibits no difference between flight and control tissues, the autoradiogram shows a substantially reduced binding to RII (Fig. 4B, lanes 6-9). Note also that both control and flight tissue samples show a faster moving autoradiographic label, presumably a proteolytic degradation product.

Photoaffinity labeling with 8-N₃ cAMP of soluble cell fractions and the particulate fraction extracts was undertaken to determine the cellular distribution of cAPK R subunits and to compare the compartmental distribution between flight tissues and controls. Total 8-N₃ cAMP bound to proteins is shown in Fig. 2, as counts per minute per mg protein. Generally the cytoplasmic fraction proteins are more extensively (3 to 4 fold) labeled than the particulate fraction proteins. In the soluble fraction no significant difference was observed between flight and controls (first three points shown in Fig. 2). In the particulate fraction extract, the flight heart muscle showed a significant increase in bound 8-N₃ cAMP, when compared to vivarium control. Similarly, the synchronous control showed an increase of total 8-N₃ cAMP binding in the particulate fraction.

Comparison of banding patterns and cyclic AMP-binding properties between soluble and particulate cell fractions of the synchronous controls is shown in Fig. 3. Electrophoretic protein banding patterns are shown in Fig. 3A and differ between the soluble and particulate cell fractions (lanes 1-4 and 6-10, respectively). The banding patterns of the soluble or particulate fractions are not different from those of either the vivarium controls or the flight animals (not shown). This is consistent with our earlier observations. The autoradiographic results, (Fig. 3B) on the other hand, show marked differences of R subunit type and distribution. The soluble fraction contains both RI and RII, although RII should be less than RI (10-15). The particulate fraction contains more RII than RI which is also consistent with previous observations. The particulate fraction contains largely RII. In sample 6, very little RII can be seen and may be due to variation between individual animals. When compared to controls, however, the extent of labeling is significantly more than in flight animals. Thus the electrophoretic and autoradiographic determination of R

subunit presence and distribution does not represent all the label that is incorporated, since the flight particulate fraction contains markedly diminished or absent R's in the cell fractions of animals from the Cosmos flight (fig. 4B). The banding patterns of the particulate samples are shown in Fig. 4A (lanes 2-5 are controls, lanes 6-9 are flight). Lane 1 is a control sample of heart tissue taken from a laboratory rat taken at the time of the experiment to test labeling specificity by adding cold cyclic AMP. Lane 6 is a color standard to show relative mobilities. The autoradiogram of the Western blot is shown in Fig. 4B. The soluble fraction contains mainly RI and a faster moving component and no differences are seen between flight and control animal samples of heart tissue extracts, Fig. 4C. As stated previously, the R subunits in the particulate fraction are mainly RII with some RI present and occasionally a faster moving fragment is seen. These fragments are probably products of proteolysis. This might also explain the increase of total counts in the synchronous simulation samples, indicating that more label per total protein may be present due to increase in the protein degradation, but not necessarily due to increased/decreased amounts of intact RII.

DISCUSSION

A major mechanism of cellular regulation is the cyclic interconversion of enzymes between the phospho- and dephosphoforms. Phosphorylation is the most common molecular regulatory mechanism - more than other covalent modification. Desensitization of the Beta receptor (adenylate cyclase system) results from continued stimulation by catecholamine hormones. This is an adaptive mechanism which may ultimately be expressed in decreased cAPK subunit synthesis and agonist-induced desensitization of the b-adrenergic receptor-linked adenylate cyclase. Pharmacological Reviews and the corresponding intracellular signal processing events have been thoroughly reviewed (Harden, T.K. Pharmacological Reviews, 35:5-28, 1983 and references therein).

Many hormones act on responsive cells by activating second messenger pathways. Of these the cyclic AMP (and the calcium) pathways change cellular activity through specific protein kinase. By phosphorylating cytoplasmic and nuclear proteins this kinase coordinates cellular activity. Biosynthesis of specific proteins is known to be modulated in heart muscle as well as in other cell types. It has now been shown that transcriptional regulation requires a cAMP response element (CRE) which is conserved in cAMP responsive genes. Phosphorylation of CRE-binding proteins may be the mechanism of gene activation in hormonally regulated cells. Consequently the relative cellular disposition of cyclic AMP-dependent protein kinase may be an index of such events in heart muscle. The results of this study appear to be related to these phenomena and should be further investigated from the molecular biology standpoint.

CONCLUSIONS

The basic signal processing of b-adrenergic stimulation is via the adenylate cyclase system via cyclic AMP-mediated intracellular events. Indices of these events are measures of cyclic AMP-dependent protein kinase activity and distribution. While catalytic activity measurements are difficult in frozen tissues, the photoaffinity labeling of cAPK R subunits can be reliably carried and used to determine relative amounts and cellular distribution of these proteins. This method of labeling cAPK R subunits using both a photoaffinity and an immunological probe was applied to heart muscle tissue of rats from the Cosmos 1887 flight.

Rat heart ventricular tissue fractionation and R subunit labeling revealed a normal (compared to control) distribution of R subunits in the soluble cell fractions and a decrease in R subunits in the particulate cell fractions. Interpretation of these data must necessarily be conservative. First, the findings are observational, based on single (individual flight) observations. Second, no precise controls are available to compare results between flights (e.g., SL-3 to Cosmos 1887).

Changes due to gravitational effects on the heart muscle under space conditions are apparent in experimental animals. These changes are occasionally observed on a morphologic basis and can be quantitated using biochemical and immunocytochemical methods.

ACKNOWLEDGEMENTS

This study was in part carried out in the Space Physiology Branch, Life Sciences Division, NASA, Ames Research Center, Moffett Field, CA, and was completed in the Laboratory of Prof. R.A. Jungmann (NIH Grant #GM 23895), Department of Molecular Biology, Northwestern University Medical School, Chicago, IL. The expert technical assistance of Mrs. Katharine Kato, Ms. Joann Stevenson and Mr. Michael Penn is acknowledged. The contributions of Mr. Penn for maintaining computer files and statistical analysis of the data are gratefully acknowledged, as is the assistance of Mr. Monte Swarup (NIH/NCI, Laboratory of Tumor Immunology, Cellular Biochemistry Section) for computer analysis and graphing the protein data.

We thank Dr. Joanna Kwast-Welfeld for her gift of the antiserum. The completion of this study was in part due to the generous support, encouragement and advice given by Dr. A.R. Hand (NIH, NIDR).

REFERENCES

1. Bendayan, M. and Zollinger, M. Ultrastructural localization of antigenic sites on osmium-fixed tissues applying the protein A-gold technique. *J. Histochem. Cytochem.* 31:101-109 (1983).
2. Benovic, J.L., Pike, L.J., Cerione, R.A., Staniszewski, C., Yoshimasa, T., Codina, J., Caron, M.G. and Lefkowitz, R.J. Phosphorylation of the mammalian beta- adrenergic receptor by cyclic AMP-dependent protein kinase. *J. Biol. Chem.* 260:7094-7101 (1985).
3. Bhalla, R.C., Gupta, R.C. and Shroa, R.V. Distribution and properties of cAMP-dependent protein kinase isozymes in the myocardium of spontaneously hypertensive rat. *J. Mol. Cell Cardiol.* 14:33-39 (1982).
4. Blomquist, G., Mitchell, J.H. and Saltin, B. Effects of bed rest on the transport system in hypogravic and hypodynamic environments. (R.H. Murray and M. McCally, eds.) NASA SP-269, Washington, DC (1969).
5. Bonder-Petersen, F., Suzuki, Y., Saduoto, T. and Christensen, N.J. Cardiovascular effects of simulated zero gravity in humans. *Acta Astronautica* 10:657-661 (1983).
6. Bungo, M.W. and Johnson, P.C. Cardiovascular examination and observations of deconditioning during the space shuttle orbital flight test program. *Aviat. Space Env. Med.* 54:1001-1002 (1983).
7. Greengard, P. Phosphorylated proteins as physiological effectors. *Science* 199:146-152 (1978).
8. Hover, P., Owens, J. and Haley, B. Use of nucleotide photoaffinity probes to elucidate molecular mechanisms of nucleotide-regulated phenomena. *Ann. N.Y. Acad. Sci.* 346:280-301 (1980).
9. Karapu, V.Y. and Ferents, A.I. Effects of hypokinesia and physical loading on cardiac myocyte ultrastructure. *Arkhiv Anatomia, Gistologii I Embriologii (NASA TM-76179 28-37 (1979))*.

10. Keely, S.L., Corbin, J.D. and Park, C.R. Regulation of adenosine 3',5'-monophosphate-dependent protein kinase. *J. Biol. Chem.* 250:4832-4840 (1975).
11. Kranias, E.G., Garvey, J.L., Srivastava, R.D. and Solaro, R.J. Phosphorylation and functional modification of sarcoplasmic reticulum and myofibrils in isolated rabbit hearts stimulated with isoprenaline. *Biochem. J.* 266:113-121 (1985).
12. Kvetansky, R. and Tigranayan, R.A. Epinephrine and norepinephrine concentrations in rat cardiac ventricles and atria after flight aboard Cosmos-1120 biosatellite. *Kosmicheskaya Biologiya I Aviakosmicheskaya Meditsina* 16:(4) 87-89 (1982).
13. Lindeman, J.P. and Watanabe, A.M. Phosphorylation of phospholamban in intact myocardium. Role of Ca⁺-calmodulin-dependent mechanisms. *J. Biol. Chem.* 260:4516-4525 (1985).
14. Lohmann, S.M., DeCamilli, P., Eining, I. and Walter, U. High-affinity binding of the regulatory subunit (RII) of cyclic AMP-dependent protein kinase to microtubule-associated and other cellular proteins. *Proc. Natl. Acad. Sci. USA* 81:6723-6727 (1984).
15. Lohmann, S.M. and Walter, U. Regulation of the cellular and subcellular concentrations and distribution of cyclic nucleotide-dependent protein kinases. *Adv. Cyclic Nuc. Prot. Phos. Res.* 18:63-117 (1984).
16. Mednieks, M.I. and Hand, A.R. Cyclic AMP-dependent protein kinase in stimulated rat parotid gland cells: compartmental shifts after in vitro treatment with isoproterenol. *Eur. J. Cell Biol.* 28:264-271 (1982).
17. Mednieks, M.I. and Hand, A.R. Nuclear cAMP-dependent protein kinase in rat parotid acinar cells. *Exp. Cell Res.* 149:45-55 (1983).
18. Mednieks, M.I. and Hand, A.R. Salivary gland ultrastructure and cyclic AMP-dependent protein kinase reactions in Space Lab-3 rats. *Am. J. Physiol. (Reg. Int. Comp. Physiol., 21)* 252:R233-239 (1987).
19. Mednieks, M.I., Jungmann, R.A. and Hand, A.R. Immunogold localization of the type II regulatory subunit of cyclic AMP-dependent protein kinase. *J. Histochem. Cytochem.* 37:339-346 (1986).
20. Mednieks, M.I., Fine, A.S., Oyama, J. and Philpott, D.E. Cardiac muscle ultrastructure and cyclic AMP reactions to altered gravity conditions. *Am. J. Physiol. (Reg. Int. Comp. Physiol., 21)* 252:R227-232 (1987).
21. Mednieks, M.I., Jungmann, R.A. and Hand, A.R. Ultrastructural immunocytochemical localization of cyclic AMP-dependent protein kinase subunits in rat parotid acinar cells. *Eur. J. Cell Biol.* 44:308-317 (1987).
22. Musacchia, X.J., Deavers, D.R., Meninger, G.A. and Davis, T.P. A model for hypokinesia effects on muscle atrophy in the rat. *J. Appl. Physiol. Respirat. Environ. Physiol.* 48:479-486 (1980).
23. Philpott, D.E., Fine, A., Kato, K., Egnor, R., Cheng, L. and Mednieks, M. Microgravity changes in heart structure and cyclic-AMP metabolism. *The Physiologist* 28:S209-210 (1985).

24. Popovic, V. Antiorthostatic hypokinesia and circulation in the rat. *The Physiologist* 24:15-16 (1981).

25. Sandler, H. Cardiovascular responses to weightlessness and prolonged bed rest. In: *A Critical Review of the U.S. and International Research on Effect of Bed Rest on Major Body Systems*. (Nicogossian, A.E. and Lewis, C.S. eds.). Washington, DC, NASA, 3-80 (1982).

TABLE I

Protein Concentration of Homogenates of Rat Heart Tissue

Protein concentration mg/ml

Sample number	Control	Simulated	Flight
1	0.65	0.65	0.67
2	0.74	0.78	0.65
3	0.74	0.75	0.68
4	0.88	0.86	0.61*
5	0.85	0.87	0.45*

Standard error calculation showed that values marked with a star (*) differ significantly from the average values of controls.

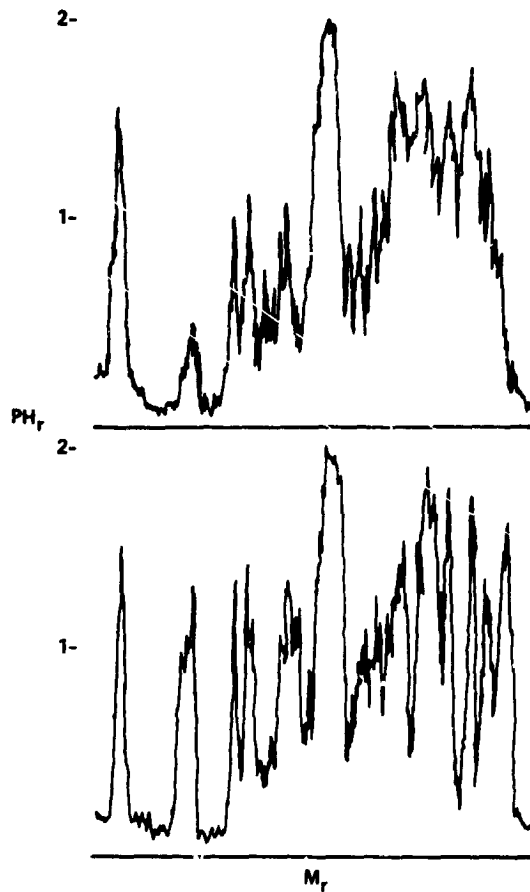


Fig. 1. Protein banding patterns of rat heart tissue fractions resolved on SDS-PAGE. The soluble fractions of a control and flight (panel A and B, respectively) are representative and contain 15-20 major bands. The axes are: relative peak height (Pr) on the ordinate and relation mobility (Mr) on the abscissa.

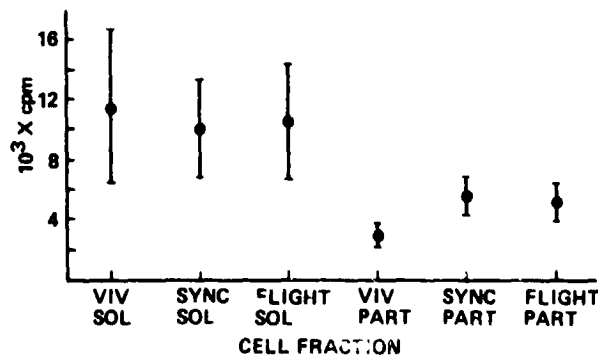


Fig. 2. Incorporation of 8-N₃ cAMP into total cell fraction protein. Photoaffinity labeling was carried out as described in Methods and the proteins were precipitated with trichloroacetic acid. Total incorporation as cpm per mg proteins are shown in the three experimental groups (control-viv; synchronous control-sync and flight) of both soluble and particulate (sol, part) cell fractions.

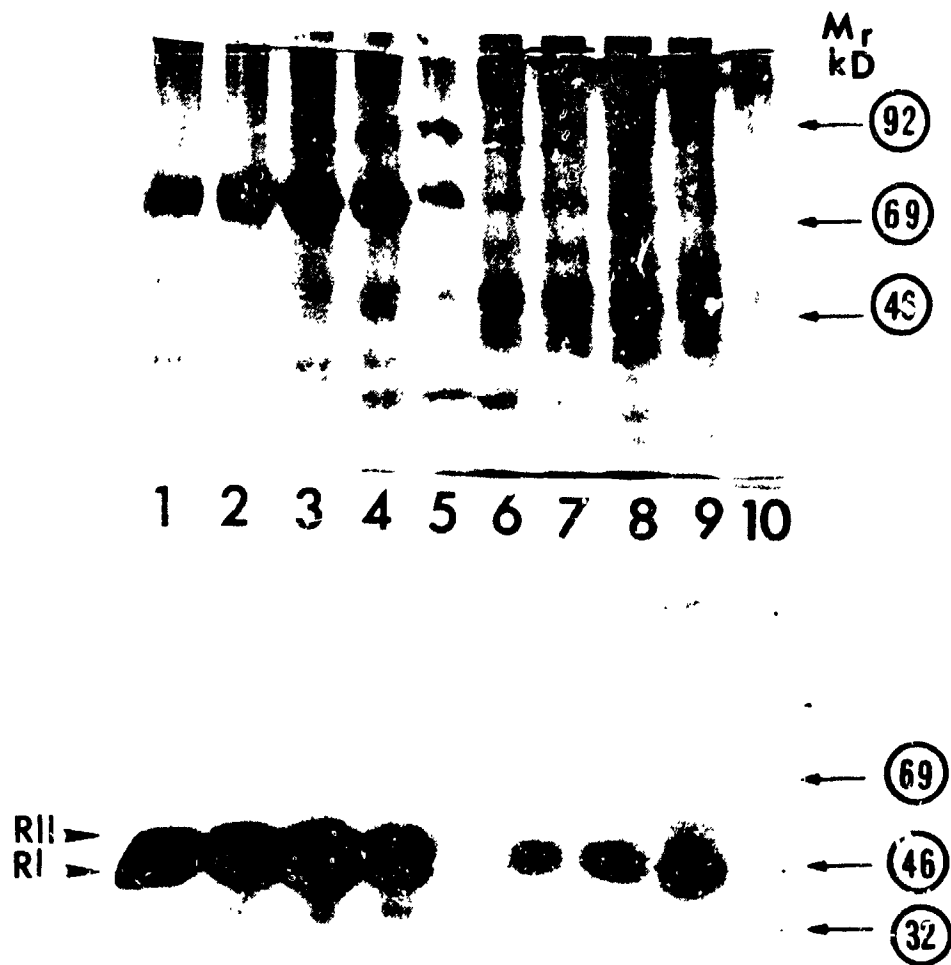


Fig. 3. Comparison of banding patterns and R subunit distribution between soluble and particulate fractions of the flight group heart muscle cell fractions. Fig. 3-A, protein banding patterns of soluble (lanes 1-4) and particulate (lanes 6-10) cell fractions. Lane 5 contains standard protein markers from which relative mobilities, shown on the right ordinate have been calculated. Fig. 3-B, autoradiogram of western-blotted, electrophoretically separated protein shown in Fig. 3-A. Lanes 1-4 soluble heart muscle cell fraction R subunit distribution. Lanes 6-9 corresponding particulate fraction, lane 10 the sample was treated in the presence of cold cyclic AMP to demonstrate specific reduction in labeling.

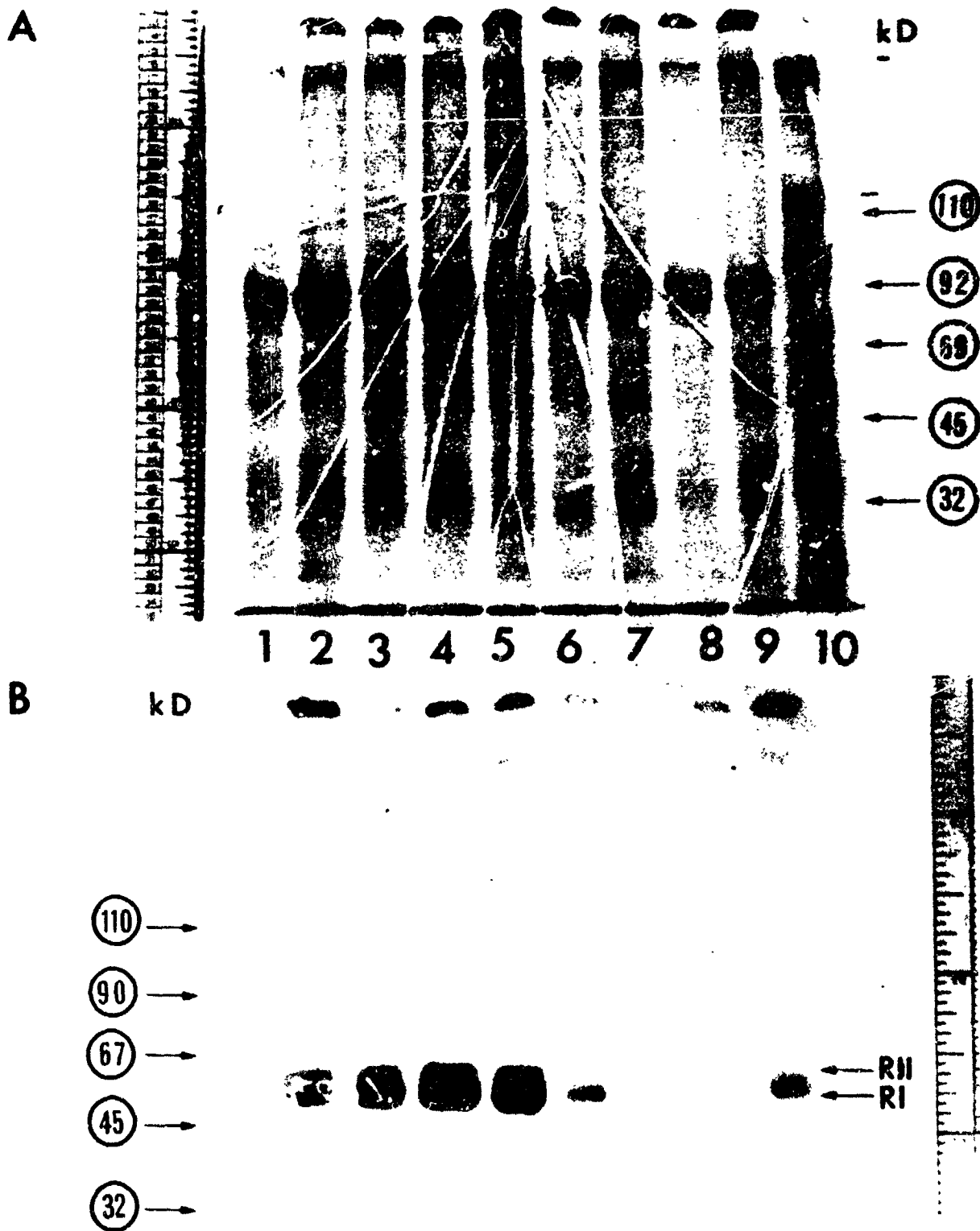


Fig. 4. Autoradiogram of particulate cell fraction of rat heart cells. Fig. 4-A, banding patterns, and Fig. 4-B, autoradiogram. Lane 1, cold competition control; lanes 2-5, controls; lanes 6-9, flight; lane 10, protein standards.

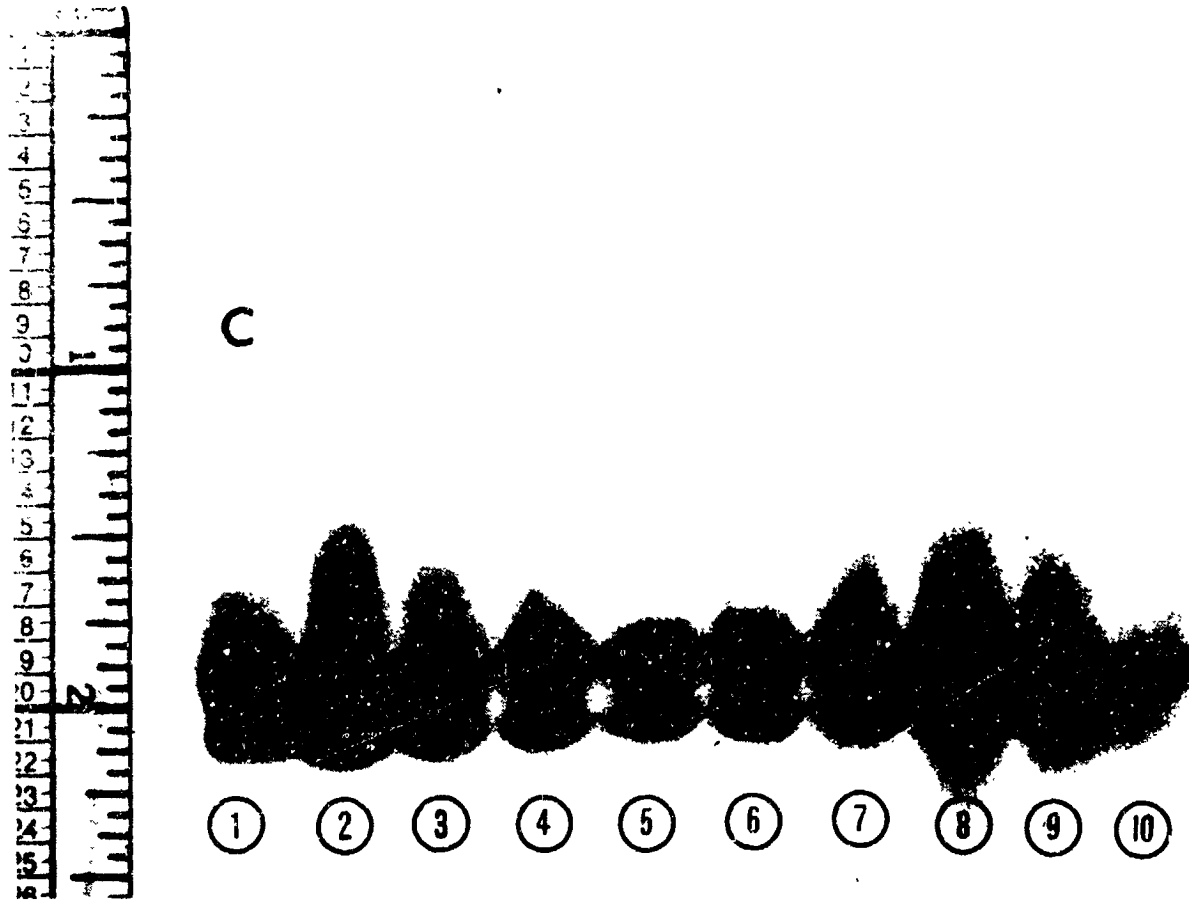


Fig. 4. Concluded. Fig. 4-C, autoradiogram of photoaffinity labeled soluble fractions of control and flight group heart muscle. Lanes 2-5, control; lanes 6-9, flight; lane 1, NIH control; lane 10, preincubated with cold cyclic AMP.

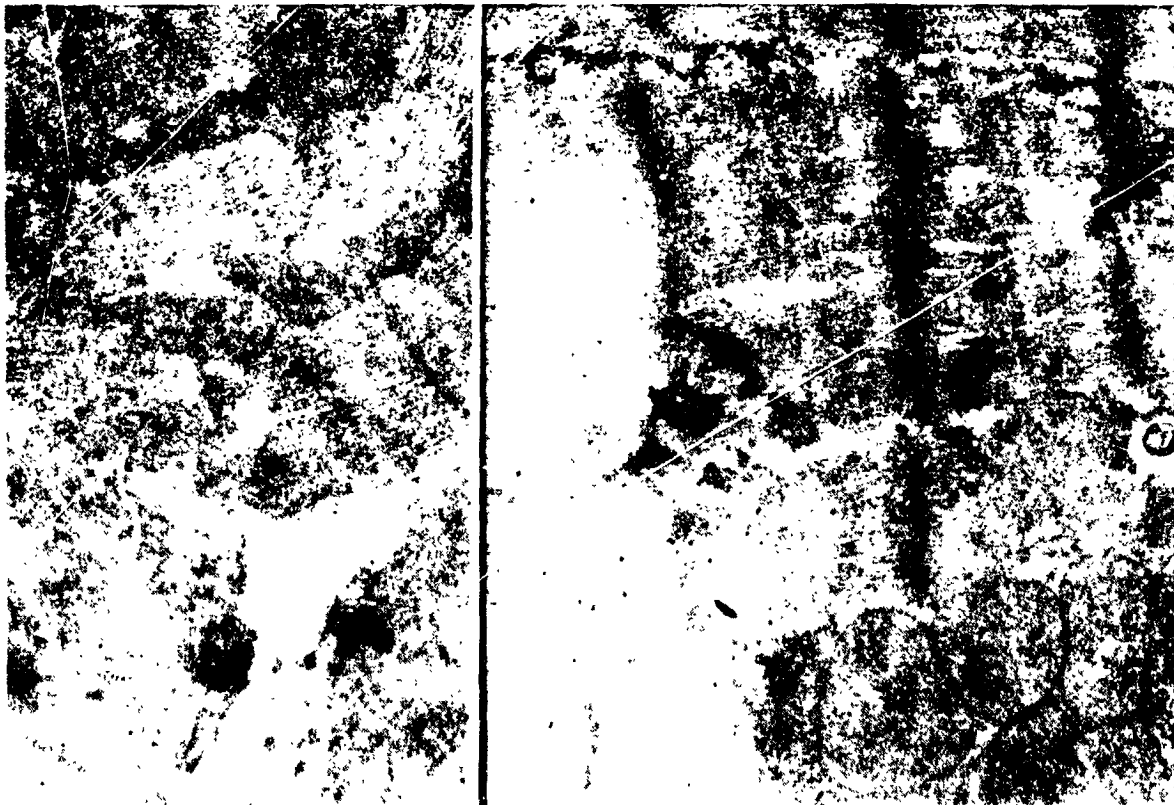
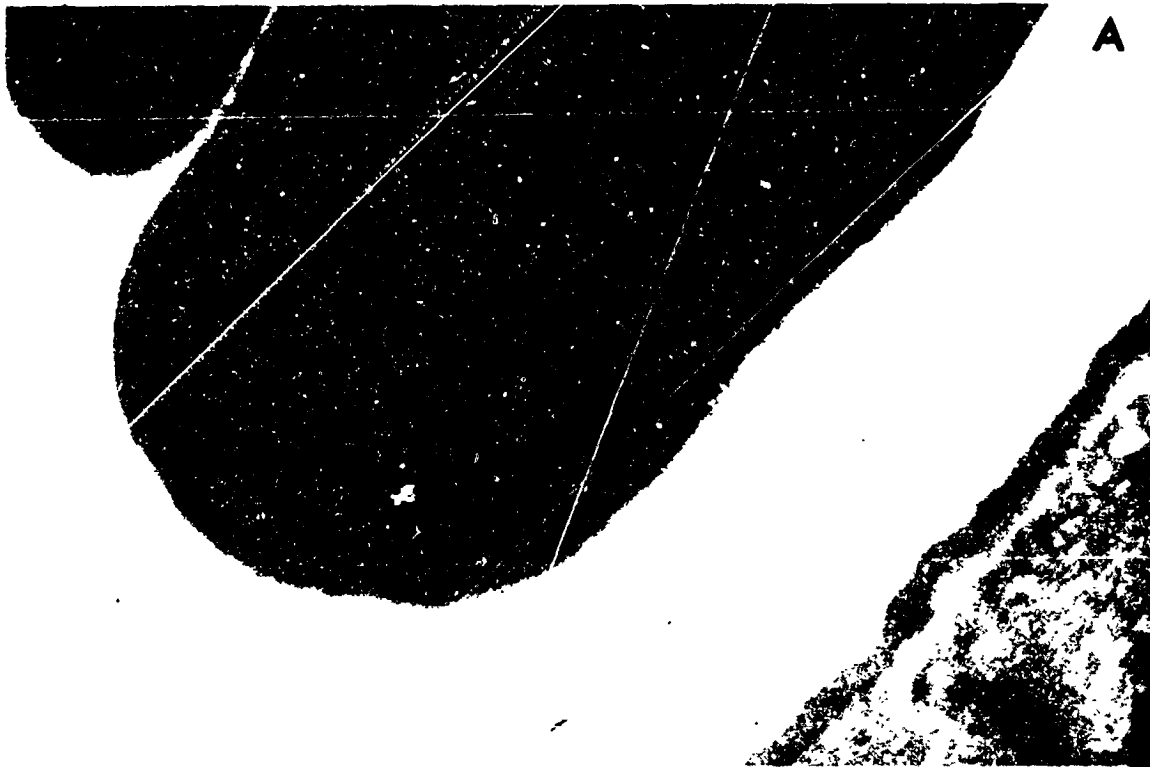


Fig. 5. Distribution of anti-RI antibody in cardiomyocytes showing electron microscopic immunogold labeling. Fig. 5-A, cross section of a blood vessel, contains a red blood cell and adjacent cardiomyocyte with gold particles (x42,500). Figs. 5-B and 5-C, heart tissue showing a comparison of flight and control animal cells (x27,500).